Applying Quality-by-Design to a coffee freeze-drying process

Applying Quality-by-Design to develop a coffee freeze-drying process

Davide Fissore, Roberto Pisano, Antonello A. Barresi

Dipartimento di Scienza Applicata e Tecnologia

Politecnico di Torino

corso Duca degli Abruzzi 24, 10129 Torino (Italy)

Abstract

This paper aims at investigating the design of a freeze-drying cycle taking into account the energy utilization efficiency. A coffee freeze-drying process is considered as case study. The analysis is focused on the primary drying, as this stage accounts for most of the energy consumption. A simplified mathematical model is used to calculate the design space of the process, with the goal to point out the operating conditions (temperature of the heating shelf and pressure in the drying chamber) that allow satisfying the constraints of the process. Experimental investigation is required to determine model parameters, namely the coefficient of heat transfer to the product, and the resistance of the dried cake to vapor flow. The same model, coupled with equations describing the dynamics of the freeze-dryer, is used to carry out the exergy analysis of the process, thus pointing out the operating conditions that allow minimizing the exergy losses and maximizing the exergy efficiency.

Keywords

Freeze-drying, coffee, quality by design, design space, process optimization, exergy.

Introduction

Among various drying processes, freeze-drying is generally recognized to allow obtaining a higher quality product, that can be easily rehydrated and retain organoleptic properties, mainly as a consequence of the low operating temperatures. In fact, the product is generally placed over the shelves of the drying chamber, where it is initially cooled at low temperature (e.g. -50°C) in such a way that most of the water freezes (the "free water"). Then, pressure in the chamber is lowered in such a way that ice sublimation can occur (primary drying). This requires supplying heat to the product as ice sublimation is an endothermic process: in pilot-scale and industrial-scale units the product is heated using a technical fluid that flows inside the shelves of the chamber. Afterwards, product temperature is increased (and, sometimes, the pressure in the drying chamber is further reduced) in order to enhance desorption of the "bound" water (secondary drying), so that the target value of residual moisture in the product can be achieved (see, among the others, Mellor, 1978; Jennings, 1999; Oetjein and Haseley, 2004; Franks, 2007).

One of the drawbacks of the freeze-drying process is that the amount of energy required is very large: although the heat of sublimation is about the same as the heat of evaporation, the amount of energy required in a freeze-drying process is higher with respect to other drying process, in case the whole process and equipment are considered (Flink, 1977). With this respect, the most critical step is primary drying, that accounts for about 45% of the total energy required by the process (Ratti, 2001).

The problem of the optimization of the primary drying stage has been widely addressed in the scientific literature with the goal to identify the values of the temperature of the heating fluid (T_{fluid}) and of the pressure in the drying chamber (P_c) that allow minimizing the drying time. In this framework there are two constraints that must be satisfied. The first is about

product temperature, that has to remain below a limit value in order to preserve product structure (i.e. to avoid dried cake collapse) and to avoid product degradation: the limit temperature is generally assumed to be few degrees higher than the glass transition temperature. On the other hand, it is necessary to avoid the loss of pressure control in the drying chamber due to the occurrence of sonic flow (choking flow) in the duct connecting the chamber to the condenser when sublimation flux is too high (Searles, 2004; Nail and Searles, 2008; Patel et al., 2010a).

The optimization problem can be solved in-line, by using a suitable monitoring and control system (Pisano et al., 2010, 2011a; Fissore and Barresi, 2011; Fissore et al., 2012): mathematical modeling is required both to calculate the values of the manipulated variables (with the goal to achieve the aforementioned goals), and to estimate the state of the system on the basis of the available measurements. Mathematical modeling can also be used to calculate off-line the design space of the primary drying, thus determining the optimal values of the operating conditions by means of a true quality-by-design approach (Giordano et al., 2011; Fissore et al., 2011a; Pisano et al., 2013).

Despite the large amount of energy required by the process, little work has been done on this aspect. To this purpose the exergy concept can be very useful. Exergy is defined as the maximum amount of work that can be extracted from a physical system by exchanging matter and energy with large reservoirs at reference states. The exergy is thus a measure of energy quality and can be associated with the irreversibilities occurring during the freeze-drying process. The goal of the exergy analysis is to identify the operating conditions that allow minimizing the exergy losses in the process because this would improve the economic efficiency (and the sustainability) of the process by increasing the efficiency of energy utilization. In the field of freeze-drying processes, Liapis and Bruttini (2008) and Liu et al. (2008) carried out a detailed exergy analysis of the various stages of the operation (freezing,

primary and secondary drying) as well as of vacuum pumping and of vapor condensing.

Liapis and Bruttini (2008) carried out the investigation using a detailed bi-dimensional model. Unfortunately, multi-dimensional models are complex, the numerical solution is time-consuming, and they involve a lot of parameters whose values is quite often unknown, and could be determined only with high uncertainty, thus impairing the accuracy of the model. Moreover, it appears from published data (Pikal, 1985; Sheehan and Liapis, 1998) that radial thermal gradients are small, even in case the product is heated by radiation from drying chamber walls, and, thus, a simple one-dimensional model is suitable to describe the dynamics of the product.

Liu et al. (2008) used a mono-dimensional model of the process, but some of the simplifying assumptions appear to be erroneous, e.g. that the vapor pressure at the sublimation interface is equal to the chamber pressure, or that the temperature of the product and the sublimation flux remain unchanged during primary drying.

In this paper a simplified approach will be used to carry out the exergy analysis of the process, using the mono-dimensional model of Velardi and Barresi (2008) to describe ice sublimation in the product, and a simple model to describe the dynamics of water vapor (and of the inert gas, in case controlled leakage is used to regulate chamber pressure) in the freeze-dryer. The goal of the study is to merge the results obtained through the design space of the process, with those obtained from the exergy analysis. As a lot of calculations are required, due to the fact that it is necessary to repeat the exergy analysis for all the potential values of T_{fluid} and P_c that could be used to carry out the process, the time required by the calculations is an important issue, and the use of simplified models is mandatory. Nevertheless, care must be paid when doing simplifying assumptions as they can significantly affect the accuracy of the results.

The case study that will be considered in the following is the freeze-drying of a coffee

extract in trays. This is due to the fact that coffee is the most common freeze-dried liquid in the food industry as this process allows preserving the coffee flavour to a great extent. At first, experimental investigation is required to determine model parameters, than, results obtained from design space calculation and exergy analysis are used to identify the best operating conditions.

Materials and Methods

Mathematical modeling

In order to describe the dynamics of the product being freeze-dried, i.e. the evolution of the temperature of the product and of the residual amount of ice, as a function of the operating conditions (T_{fluid} and P_c) it is necessary to model the dependence of the heat flux to the product and of the mass flux from the sublimation interface on the operating conditions (see Figure 1). Generally, the heat flux from the heating fluid to the product is described by the following equation:

$$J_q = K_v \left(T_{fluid} - T_B \right) \tag{1}$$

where T_B is the temperature of the product at the bottom of the tray (or of the container used), and K_v is a heat transfer coefficient that accounts for the various mechanisms of heat transfer to the product. The coefficient K_v depends on the characteristics of the container and of the equipment, and on chamber pressure (Pikal, 1984, 1985; Pisano et al., 2011b). The following equation is generally proposed in the literature to describe pressure dependence of K_v:

$$K_v = A_{K_v} + \frac{B_{K_v} \cdot P_c}{1 + C_{K_v} \cdot P_c} \tag{2}$$

The solvent flux from the interface of sublimation to the drying chamber can be calculated

using the following equation:

$$J_w = \frac{1}{R_p}\left(p_{w,i} - p_{w,c}\right) \tag{3}$$

where $p_{w,i}$ and $p_{w,c}$ are, respectively, the partial pressure of water vapor at the interface of sublimation and in the drying chamber, and R_p is the dried cake resistance to vapor flux. R_p is a function of product characteristics and of the thickness of the dried layer and, generally, the following equation is proposed:

$$R_p = A_{R_p} + \frac{B_{R_p} \cdot L_{dried}}{1 + C_{R_p} \cdot L_{dried}} \tag{4}$$

To calculate the equilibrium vapor pressure, that is a function of the interface temperature, the equation proposed by Goff and Gratch (1946) can be used. Values calculated using this equation are is in good agreement with data reported by Wagner et al. (1994) and with experimental values reported by Marti and Mauersberger (1993).

The simplified one-dimensional model proposed by Velardi and Barresi (2008) can be used to describe the dynamics of the process. It is composed by the energy balance for the frozen product and the mass balance for the water vapor inside the dried product. The slow dynamics of the process allows neglecting the energy accumulation in the frozen product, and the mass accumulation in the dried layer. The presence of an inert gas in the product is neglected, as well as the contribution to heat transfer of the side wall of the container.

The apparatus can be described as two units in series, the drying and condenser chamber, connected by a short duct (Sane and Hsu, 2008). The convective flow that passes in the duct can be described as follows:

$$N_{duct} = k_{duct}\left(P_c - P_{cond}\right) \tag{5}$$

where k_{duct} is the permeability of the drying chamber-condenser connection. Its dependence on the total flow rate can be described by means of a polynomial function whose coefficients

should be experimentally identified for the apparatus used:

$$k_{duct} = a_0 + a_1 N_{duct} + a_2 N_{duct}^2 \tag{6}$$

The material balance for the drying and condenser chamber can be written assuming that the gas is made of water and other gas (e.g. nitrogen and oxygen, due to leakage and controlled leakage for pressure control). Thus, the material balance equations for the drying chamber result:

$$\frac{dn_{w,c}}{dt} = A_{sub}\frac{J_w}{M_w} + y_{w,l}N_l - y_{w,c}N_{duct} \tag{7}$$

$$\frac{dn_c}{dt} = A_{sub}\frac{J_w}{M_w} + N_l + N_{cl} - N_{duct} \tag{8}$$

where N_l is the leakage flow rate, N_{cl} is the controlled leakage flow rate, $y_{w,c}$ is the water molar fraction in the drying chamber, $y_{w,l}$ is the water molar fraction in the leakage stream, $n_{w,c}$ is the number of water moles in the chamber, and n_c is the total number of moles of gas in the chamber. Assuming that the gas behaves as an ideal gas, the dynamics of gas composition and of the total chamber pressure is described by the following equations:

$$\frac{dy_{w,c}}{dt} = \left(\frac{RT_c}{P_c V_c}\right)\left(A_{sub}\frac{J_w}{M_w} + y_{w,l}N_l - y_{w,c}N_{duct}\right) \tag{9}$$

$$\frac{dP_c}{dt} = \left(\frac{RT_c}{V_c}\right)\left(A_{sub}\frac{J_w}{M_w} + N_l + N_{cl} - N_{duct}\right) \tag{10}$$

The inlet flow rate of inert gas (N_{cl}) is calculated depending on P_c as follows:

$$\begin{aligned} &P_c - P_{c,sp} = 0 \qquad && N_{cl}^{t(i)} = N_{cl}^{t(i-1)} \\ &P_c - P_{c,sp} > 0 \qquad && N_{cl}^{t(i)} = N_{cl}^{t(i-1)} - \Delta N_{cl}\left(P_c^{(i)} - P_{c,sp}\right) \\ &P_c - P_{c,sp} < 0 \qquad && N_{cl}^{t(i)} = N_{cl}^{t(i-1)} + \Delta N_{cl}\left(P_c^{(i)} - P_{c,sp}\right) \end{aligned} \tag{11}$$

where $P_{c,sp}$ is the set-point of chamber pressure and $N_{cl}^{t(i)}$ is the value of controlled leakage flow rate at the *i*-th time instant, calculated on the basis of the pressure at that time instant ($P_c^{(i)}$) and of the controlled leakage flow rate in the previous time instant.

The transient material balance for the chamber condenser is given by the following equations:

$$\frac{dn_{w,cond}}{dt} = y_{w,c}N_{duct} - y_{w,cond}N_{pump} - N_{ice} \tag{12}$$

$$\frac{dn_{cond}}{dt} = N_{duct} - N_{pump} - N_{ice} \tag{13}$$

where N_{ice} is the molar flow rate of water that is trapped in the condenser as ice, N_{pump} is the flow rate of gas evacuated by the vacuum pump, $y_{w,cond}$ is the water molar fraction in the condenser chamber, $n_{w,cond}$ is the number of water moles in the condenser chamber, and n_{cond} is the total number of moles of gas in the condenser chamber. Also in this case, assuming an ideal gas behavior, equations (12) and (13) can be written as:

$$\frac{dy_{w,cond}}{dt} = \left(\frac{RT_{cond}}{P_{cond}V_{cond}}\right)\left(y_{w,c}N_{duct} - y_{w,cond}N_{pump} - N_{ice}\right) \tag{14}$$

$$\frac{dP_{cond}}{dt} = \left(\frac{RT_{cond}}{V_{cond}}\right)\left(N_{duct} - N_{pump} - N_{ice}\right) \tag{15}$$

It is possible to assume that all the water vapor that reaches the condenser chamber is condensed, and the residual water in the gas phase corresponds to the equilibrium value at the temperature of the cooling surface. With respect to vacuum pump, the flow rate of gas evacuated is a function of the inlet pressure of the pump, i.e. the total pressure of the condenser chamber. Hence, equations (14) and (15) can be solved only if the characteristic curve of the vacuum pump is known.

Model parameter determination

The gravimetric test was used to determine the value of K_v at a given pressure: the tray was filled with water and, then, the primary drying was carried out for a time interval Δt. If Δm is the measured weight loss during the test, than:

$$K_v = \frac{\Delta m \cdot \Delta H_s}{\Delta t \cdot \left(T_{fluid} - T_B\right) \cdot A_{sub}} \tag{16}$$

As it appears from eq. (16) ice temperature at the bottom has to be measured during the test. The gravimetric test was repeated at three different values of P_c with the goal to determine the values of the parameters appearing in eq. (2) looking for best fit between measured and calculated values of K_v at different values of P_c.

With respect to the parameter R_p, it was determined using the pressure rise test: the valve in the duct connecting the drying chamber to the condenser is closed for a short time interval during primary drying, thus causing pressure increase in the chamber. A mathematical model is used to calculate the pressure rise, and model parameters that give best fit between model predictions and experimental measurements are calculated. DPE+ algorithm has been used to this purpose (Fissore et al., 2011b). The equilibrium water pressure ($p_{w,i}$) is calculated looking for best fit between calculated and measured values of chamber pressure, solving the least-square problem:

$$\min_{T_{i,0}} \sum_k \left(P_{c,k} - P_{c,meas,k}\right)^2 \tag{17}$$

The steps required by DPE+ algorithm are the followings:

1. Initial guess of $T_{i,0}$, product temperature at the sublimation interface at the beginning of the test (i.e. when $t = t_0$);
2. Calculation of $p_{w,i,0}$ when product temperature is $T_{i,0}$. The Goff-Gratch equation (Gogg and Gratch, 1946) can be used to this purpose;
3. Calculation of the first derivative of the pressure rise curve at $t = t_0$;
4. Calculation of R_p using the following equation:

$$R_p = \frac{N_v A_p R T_c}{V_c M_w} \left(\frac{dp_{w,c}}{dt}\right)^{-1}_{t=t_0} \left(p_{w,i,0} - p_{w,c,0}\right) \tag{18}$$

5. Calculation of J_w using the following equation:

$$J_w = \frac{1}{R_p}\left(p_{w,i,0} - p_{w,c,0}\right) \tag{19}$$

6. Determination of L_{frozen} integrating numerically the mass balance for the frozen layer:

$$\frac{dL_{frozen}}{dt} = -\frac{1}{\rho_{frozen} - \rho_{dried}} J_w \tag{20}$$

7. Determination of K_v from the energy balance at the interface of sublimation:

$$J_q = \Delta H_s J_w \tag{21}$$

(where J_q is given by eq. (1));

8. Integration of model equation describing pressure rise in the chamber in the time interval (t_0, t_f), where $t_f - t_0$ is the time length of the test, in order to calculate $P_{c,k}$.
9. Evaluation of $T_{i,0}$ that best fits the calculated chamber pressure to the measured data.

Once the optimal value of $T_{i,0}$ has been calculated, also model parameters R_p and K_v, as well as L_{frozen} (or L_{dried}) and J_w are known. The test is then repeated during primary drying stage in order to determine the parameters appearing in eq. (4) looking for best fit between measured and calculated values of R_p at different values of L_{dried}.

Design space calculation

The design space is constituted by the set of values of T_{fluid} and P_c that maintain product temperature below the selected limit value. For a given value of chamber pressure it is possible to calculate the maximum allowable temperature of the heating fluid ($T_{fluid,max}$) using the energy balance at the interface of sublimation:

$$K_v \left(T_{fluid} - T_B \right) = \Delta H_s \frac{1}{R_p} \left(p_{w,i} - p_{w,c} \right) \tag{22}$$

Equation (22) can be written as a function of T_i:

$$\left(\frac{1}{K_v} + \frac{L_{frozen}}{k_{frozen}} \right)^{-1} \left(T_{fluid} - T_i \right) = \Delta H_s \frac{1}{R_p} \left(p_{w,i} - p_{w,c} \right) \tag{23}$$

Product temperature T_i can therefore be calculated once the values of T_{fluid}, P_c and L_{dried} are known (as $p_{w,i}$ is a function of T_i, R_p is a function of L_{dried} and $L_{frozen} = L_0 - L_{dried}$). This means that the design space changes during primary drying, as pointed out by Fissore et al. (2011a). For a given value of L_{dried} and of P_c and, thus, of K_v, the limit value $T_{fluid,max}$ is the one that brings T_i to the limit value (T_{max}):

$$T_{fluid,max} = T_{max} + \left(\frac{1}{K_v} + \frac{L_{frozen}}{k_{frozen}} \right) \Delta H_s \frac{1}{R_p} \left[p_{w,i}\left(T_{max}\right) - p_{w,c} \right] \quad (24)$$

For a given value of L_{dried} it is thus possible to calculate $T_{fluid,max}$ as a function of P_c, i.e. the design space.

Exergy analysis

During primary drying energy is required to sublimate the ice in the product. The approach of Liu et al. (2008) to calculate the exergy input and the exergy losses has been followed in this study, but using the model of Velardi and Barresi (2008) to calculate product dynamics as the validity of some of the hypothesis at the basis of the paper of Liu et al. appears to be questionable as previously pointed out.

The exergy losses due to heat transfer during primary drying ($Ex_{loss,h}^{pd}$) are calculated from the temperature profile in the dried layer (Liu et al., 2008):

$$Ex_{loss,h}^{pd} = A_{sub} \int_0^{t_d} \int_0^{L_{dried}} \frac{T_0 k_{dried}}{T^2} \left(\frac{dT}{dx} \right)^2 dx dt \quad (25)$$

where T_0 is a reference temperature, T the temperature of the product at axial position x, k_{dried} is the thermal conductivity and L_{dried} is the thickness of the dried cake, and t_d is the duration of primary drying. The temperature profile in the dried layer is calculated solving the Fourier equation written for the dried cake: the mathematical model previously described allows calculating the vapor flux entering the dried layer as well as its temperature during primary drying.

The exergy input resulting from heat transfer above the reference temperature T_0 (considering that T_0 is assumed to be equal to 0°C and, therefore, product temperature remains below this value throughout primary drying) given by (Liu et al., 2008):

$$Ex_{in,h}^{pd} = T_0 m_p c_{p,\,frozen}\left[\ln\left(\frac{T_i}{T_{freeze}}\right) - \frac{T_i - T_{freeze}}{T_0}\right] + m_p \Delta H_s \left(\frac{T_0}{T_i} - 1\right) + \\ + T_0\left(m_{w,in} - m_{w,\,fin}\right) c_{p,dried}\left[\ln\left(\frac{T_0}{T_i}\right) - \frac{T_0 - T_i}{T_0}\right] \tag{26}$$

where m_p is the mass of moist product, $m_{w,in}$ and $m_{w,out}$ are respectively the mass of water in the product at the beginning and at the end of primary drying, T_{freeze} is the product temperature at the end of the freezing stage. The equation of Liu et al. (2008) has to be modified accounting for the variation of T_i and of sublimation flux during time, thus obtaining:

$$Ex_{in,h}^{pd} = T_0 A_{sub}\int_0^{t_d}\left\{\frac{J_w}{(\omega_0 - \omega)} c_{p,\,frozen}\left[\ln\left(\frac{T_i}{T_{freeze}}\right) - \frac{T_i - T_{freeze}}{T_0}\right] + \frac{J_w}{(\omega_0 - \omega)}\Delta H_s\left(\frac{T_0}{T_i} - 1\right) + \\ + T_0 J_w c_{p,dried}\left[\ln\left(\frac{T_0}{T_i}\right) - \frac{T_0 - T_i}{T_0}\right]\right\} dt \tag{27}$$

With respect to mass transfer in the product being dried, the presence of noncondensable gases resulting from leakage and outgassing of the surfaces in the system, as well as inert gases from the material being dried, can be neglected. Thus, the exergy losses due to water vapor flux in the dried layer ($Ex_{loss,m}^{pd}$) are given by:

$$Ex_{loss,m}^{pd} = -\frac{A_{sub} T_0 R}{M_w}\int_0^{t_d} J_w \int_0^{L_{dried}}\left[\frac{1}{p_w(x)}\frac{dp_w(x)}{dx}\right] dx dt \tag{28}$$

where p_w is water vapor partial pressure at axial position x. The exergy input in the dried layer due to mass transfer ($Ex_{in,m}^{pd}$) is given by (Liu et al., 2008):

$$Ex_{in,m}^{pd} = A_{sub} T_0 \int_0^{t_d} J_w \left\{c_{p,v}\left[\frac{T_i}{T_0} - 1 - \ln\left(\frac{T_i}{T_0}\right)\right] + \frac{R}{M_w}\ln\left(\frac{p_{w,i}}{P_0}\right)\right\} dt \tag{29}$$

The vapor produced in the drying chamber arrives onto the cold surface of the condenser. The change in temperature, as well as in the state, of the vapor in the condenser can be described as follows:

- the temperature of the vapor ($T_{in,cond}$) is cooled down to the temperature that causes

desublimation of vapor (T_{des});

- the vapor desublimates at the temperature T_{des};

- the temperature of the ice decreases to reach the final value ($T_{out,cond}$).

The exergy input of the vapor condenser (Ex_{in}^{cond}) is given by (Liu et al., 2008):

$$Ex_{in}^{cond} = Q_{cond}\left(\frac{T_0}{T_{cooling}} - 1\right) \tag{30}$$

where $T_{cooling}$ is the temperature of the cooling medium, and Q_{cond}, the heat exchanged in the condenser, is given by:

$$Q_{cond} = A_{sub}\int_0^{t_d} J_w\left\{\left(T_{in,cond} - T_{des}\right)c_{p,v} + \Delta H_s + \left(T_{des} - T_{out,cond}\right)c_{p,ice}\right\}dt \tag{31}$$

The exergy losses (Ex_{loss}^{cond}) can be calculated using the following equation (Liu et al., 2008):

$$\begin{aligned} Ex_{loss}^{cond} = \left(m_{w,in} - m_{w,fin}\right)\cdot\Bigg\{ & T_0 c_{p,v}\left(\ln\frac{T_{des}}{T_{in,cond}} - \frac{T_{des} - T_{in,cond}}{T_{cooling}}\right) + \\ & + T_0\Delta H_s\left(\frac{1}{T_{cooling}} - \frac{1}{T_{des}}\right) + T_0 c_{p,ice}\left(\ln\frac{T_{out,cond}}{T_{des}} - \frac{T_{out,cond} - T_{des}}{T_{cooling}}\right)\Bigg\} \end{aligned} \tag{32}$$

Taking into account the variation of the sublimation flux with time, as well as of T_{des} due to the variation of pressure in the condenser chamber, eq. (32) can be written as:

$$\begin{aligned} Ex_{loss}^{cond} = T_0 A_{sub}\int_0^{t_d} J_w\Bigg\{ & c_{p,v}\left(\ln\frac{T_{des}}{T_{in,cond}} - \frac{T_{des} - T_{in,cond}}{T_{cooling}}\right) + \\ & + T_0\Delta H_s\left(\frac{1}{T_{cooling}} - \frac{1}{T_{des}}\right) + T_0 c_{p,ice}\left(\ln\frac{T_{out,cond}}{T_{des}} - \frac{T_{out,cond} - T_{des}}{T_{cooling}}\right)\Bigg\} dt \end{aligned} \tag{33}$$

The vacuum pump is used to reduce pressure in the drying chamber during the startup stage of the process, and to evacuate the noncondensable gases resulting from leakage (air), from controlled leakage used for pressure control (nitrogen, in most cases), and from the material being dried. The exergy input of the vacuum system is given by the power input multiplied by the drying time:

$$Ex_{loss}^{pump} = R\int_0^{t_d} N_{pump} \left\{ \frac{n}{n-1} T_{cond} \left[\left(\frac{P_{out}}{P_{cond}} \right)^{\frac{n-1}{n}} - 1 \right] \right\} dt \tag{34}$$

The exergy losses due to the compression of a perfect gas can be written as:

$$Ex_{loss}^{pump} = RT_0 \int_0^{t_d} \left[N_{pump} \ln \left(\frac{P_{out}}{P_{cond}} \right) \right] dt \tag{35}$$

Finally, it is possible to calculate the exergy efficiency in the following way:

$$\eta = \frac{\left(Ex_{in,h}^{pd} + Ex_{in,m}^{pd} + Ex_{in}^{cond} + Ex_{in}^{pump} \right) - \left(Ex_{loss,h}^{pd} + Ex_{loss,m}^{pd} + Ex_{loss}^{cond} + Ex_{loss}^{pump} \right)}{\left(Ex_{in,h}^{pd} + Ex_{in,m}^{pd} + Ex_{in}^{cond} + Ex_{in}^{pump} \right)} \tag{36}$$

Case study

The case study is the freeze-drying of a coffee extract: it was prepared using commercial freeze-dried coffee and de-ionized water obtained using a Millipore water system (Milli-Q RG, Millipore, Billerica, MA). The solute percentage in the resulting solution was equal to 25%. The glass transition temperature for this product was measured using a differential scanning calorimeter (DSC type Q200, TA Instruments, New Castle, DE, USA).

Model parameters were determined in a small-size industrial apparatus (LyoBeta25 by Telstar, Terrassa, Spain) with a free chamber volume of 0.178 m^3 and equipped with T-type miniature thermocouples, capacitance (626A Baratron, MKS Instruments, Andover, MA, USA) and thermal conductivity (Pirani PSG-101-S, Inficon, Bad Ragaz, Switzerland) gauges. In the capacitance gauge the sensing element flexes elastically under the effect of a pressure gradient across it, and this causes a change in capacitance that is measured by the gauge. In a thermoconductivity gauge a metal wire is suspended in a tube connected to the drying chamber. The temperature of the wire, and, thus, its resistance, depends on the electric current flowing through it and on the rate at which the filament loses heat to the surrounding gas, and therefore on the gas thermal conductivity, that is directly proportional to pressure at a given

temperature. Therefore, measuring the voltage across the wire and the electric current the resistance can be determined and, from this value, the pressure is measured. In the tests the pressure in the drying chamber is regulated by bleeding of inert gas as it guarantees better pressure control with respect to managing the valve on the vacuum pump. Table 1 reports some geometry features of the apparatus. The characteristic curve of the vacuum pump is given in Table 2.

The product was loaded over one of the shelves using a metallic tray (mean wall thickness = 2 mm): the mean thickness of the frozen product was equal to 12.5 mm.

Results and Discussion

As it has been outlined in the Materials and Methods section, in order to use the mathematical model for the calculation of the design space, as well as of the exergy losses during primary drying as a function of the operating conditions (T_{fluid} and P_c), model parameters (K_v and R_p) have to be determined.

Figure 2 (graph A) shows the values of the coefficient K_v measured with the gravimetric test, as well as the curve obtained when using eq. (2), whose parameters have been determined looking for best fit between calculated and measured values of the heat transfer coefficient, obtaining A_{K_v} = 1.1 W m^{-2}K^{-1}, B_{K_v} = 0.66 W m^{-2}K^{-1}Pa^{-1}, C_{K_v} = 0.005 Pa^{-1}. Figure 2 (graph B) shows the values of dried cake resistance determined with the pressure rise test and DPE+ algorithm. As is well known accurate and reliable results cannot be obtained in the second part of primary drying when using pressure-rise-test based method. Thus, only the first set of the values of R_p (the filled symbols in Figure 2 – graph B) have been considered to calculate the parameters of eq. (4) (while empty symbols indicate the wrong estimations

obtained from the pressure rise test), obtaining A_{R_p} = 2.5·10^4 m s^{-1}, B_{R_p} = 1.2·10^9 s^{-1}, C_{R_p} = 5.38·10^3 m^{-1}.

Once model parameters have been determined, model validation is required. Model validation can be carried out by comparing:

- the calculated values of product temperature with those measured by the thermocouples and those estimated with the pressure rise test and DPE+ algorithm;
- the calculated values of frozen (or dried) layer thickness with those estimated with the pressure rise test and DPE+ algorithm;
- the duration of the process estimated by the model and determined experimentally considering the ratio of the pressure signals provided by the Baratron and Pirani sensors (Armstrong, 1980; Patel et al., 2010b).

Figure 3 shows an example of the results obtained in a coffee freeze-drying cycle operated at constant values of heating fluid temperature and chamber pressure. Drying time, determined from the ratio of the pressure signals obtained from the Pirani and the Baratron sensors, ranges from 19 to 23 h (graph A). The value determined with mathematical simulation of the process is about 20 h. The agreement between the calculated dynamics of the frozen layer thickness (graph B) and of product temperature (graph C) are in fairly good agreement with the values obtained from the pressure rise test and DPE+ algorithm. With respect to product temperature, reliable values are obtained from the pressure rise test only in the first part of the primary drying. As the operating conditions are not modified and the product temperature remains below the glass transition temperature (-24.5°C), then product temperature can be supposed to remain roughly constant, until the end of primary drying, as predicted by the mathematical simulation of the process.

At this point it is possible to calculate the design space of the process, using the approach of Fissore et al. (2011a), that is based on the same model of the process previously

validated. For the product under investigation the glass transition temperature determined with DSC is -24.5°C. Results are shown in Figure 4 (graph A). The design space is affected by dried layer thickness as it changes the resistance to vapor flow and, thus, a couple of values of T_{fluid} and P_c that belong to the design space at the beginning of primary drying, may lay outside the design space when drying goes on. In case we aim to look for a simple cycle, where the values of the operating conditions are not modified during primary drying, then we need to take into account the curve of the design space calculated for a value of dried layer thickness approaching the total product thickness. Obviously, there are a lot of values of the operating conditions that allow fulfilling the constraint about maximum product temperature. In order to choose among them it is necessary to consider the values of the sublimation flux, as it is advantageous to reduce the duration of the primary drying. Figure 4 (graph B) shows the values of the sublimation flux in a certain time instant during primary drying (the trend of the curves is the same throughout the primary drying phase). Looking at the curves of Figure 4 (graph B) it comes out that the optimal operating conditions (i.e. those that maximize the sublimation flux) correspond to low values of P_c (e.g. 5 Pa in this case) and high values of T_{fluid} (e.g. -5°C in this case).

In order to assess the effect of the operating conditions in the drying chamber (T_{fluid} and P_c) on the exergy losses of the process, we performed the calculations of the exergy losses during sublimation phase for both the product in the drying chamber, the vapor condenser and the vacuum pump. Figure 5 shows the values of the exergy losses in the primary drying stage, for vapor condensing and vacuum pumping (given as percentage of the total exergy loss), for different values of P_c. It comes out that at low values of T_{fluid} most of exergy losses occur in the pump, while the contribution of the condenser and of the drying chamber increases as the temperature of the heating fluid increases. With respect to chamber pressure, the contribution

of exergy losses in the chamber decreases as chamber pressure increases, while that of vacuum pump and condenser increases.

Figure 6 shows the values of the exergy losses in the primary drying step as a function of chamber pressure and heating fluid temperature. It appears that while the shelf temperature seems to have no effect on the exergy losses in the condenser (this is due to the different contributions of the phenomena occurring in the condenser on the exergy losses, namely the cooling of the vapor to the desublimation temperature, the desublimation of the vapor, and the temperature decrease to the final value as modelled in eq. (32)), its effect is remarkable on the drying chamber losses and, in particular, the higher is the temperature of the fluid, the higher are the exergy losses as this increases product temperature: this is due to the fact that a higher surface temperature causes the temperature gradient in the dried layer to be larger. The value of the chamber pressure affects both exergy losses in the drying chamber and in the condenser, but the effect is different: while increasing chamber pressure decreases the exergy losses in the chamber, this increases the exergy losses in the condenser. The chamber pressure affects both heat transfer and mass transfer in the dried layer of the material: the temperature gradient can be decreased due to the heat transfer enhancement and this may reduce the exergy losses. On the other side, when chamber pressure increases, also the pressure gradient and, thus, the exergy losses due to mass transfer increase. In a process where heat transfer to the product strongly affects the dynamics of the system, heat transfer to the product plays a more important role in the exergy losses than mass transfer in the material does and, thus, the exergy losses decrease when increasing chamber pressure. In a mass transfer-controlled process the effect of chamber pressure would be the opposite. As the process under investigation is under heat transfer control, then exergy losses decrease when increasing chamber pressure. With respect to the condenser, when increasing chamber pressure also the

sublimation temperature increases, and this is responsible for the increase of the exergy losses.

The effect of the operating conditions on the cumulative exergy losses of the process is shown in Figure 7. It appears that the exergy losses can be minimized working at high shelf temperature and low chamber pressure. Nevertheless, we have to take into account the exergy input, and to calculate the exergy efficiency as a function of the operating conditions and the information about the exergy efficiency can be added to the design space of the product. An example of these calculations is shown in Figure 8. It comes out that the values of T_{fluid} and P_c that allows maximizing the exergy yield are, in this case, those corresponding to high values of chamber pressure and low values of shelf temperature. When designing the freeze-drying cycle a compromise has thus to be achieved, as the goals are to minimize the duration of primary drying (and, thus, to maximize the sublimation flux) and to maximize the exergy yield (i.e. to minimize the exergy losses). This is an example of the common conflict between time efficiency and Second Law energy efficiency, being an energy efficient process favored by low heating temperature and high chamber pressure.

Conclusion

The determination of the optimal freeze-drying cycle is of utmost importance as the freeze-drying process requires a large amount of energy. If only drying time is taken into account, it appears that the values of the operating conditions (T_{fluid} and P_c) that should be selected are in the upper right portion of the design space, i.e. high values of shelf temperature and low values of chamber pressure: 5 Pa and -5°C appear to be the (near) optimal operating conditions in case a simple cycle is desired (i.e. a cycle with constant values of T_{fluid} and P_c).

Exergy analysis can be effective to account for the efficiency in the use of energy. For the coffee freeze-drying process the exergy losses are minimized if high values of chamber pressure and low values of heating fluid temperature are considered: 30 Pa and -20°C are the (near) optimal operating conditions in case a simple cycle is desired.

Therefore, in order to improve the sustainability of the freeze-drying process, i.e. to maximize the energy efficiency, the best operating conditions are different from those resulting in the minimum drying time. It has to be highlighted that this result is affected by the thermal properties of the system, as well as by the values of the heat and mass transfer coefficients and, thus, different conclusions may be achieved in case the freeze-drying of different products is investigated.

Acknowledgements

The contribution of Salvatore Genco (Politecnico di Torino) for the experimental investigation is gratefully acknowledged.

Notation

A_{K_v}	parameter used in eq. (2), W $m^{-2}K^{-1}$
A_p	cross surface of the product in the vial, m^{-2}
A_{R_p}	parameter used in eq. (4), m s^{-1}
A_{sub}	total surface of sublimation, m^2
a_0	parameter used in eq. (6), kmol $Pa^{-1}s^{-1}$
a_1	parameter used in eq. (6), Pa^{-1}
a_2	parameter used in eq. (6), $kmol^{-1}Pa^{-1}s^{-1}$
B_{K_v}	parameter used in eq. (2), W $m^{-2}K^{-1}Pa^{-1}$
B_{R_p}	parameter used in eq. (4), s^{-1}
C_{K_v}	parameter used in eq. (2), Pa^{-1}
C_{R_p}	parameter used in eq. (4), m^{-1}
$c_{p,dried}$	heat capacity of the dried product, J $kg^{-1}K^{-1}$
$c_{p,frozen}$	heat capacity of the frozen product, J $kg^{-1}K^{-1}$
$c_{p,ice}$	heat capacity of the ice, J $kg^{-1}K^{-1}$
$c_{p,v}$	heat capacity of the water vapor, J $kg^{-1}K^{-1}$
Ex_{in}^{cond}	exergy input to the condenser, J
$Ex_{in,h}^{pd}$	exergy input due to heat transfer during primary drying, J
$Ex_{in,m}^{pd}$	exergy input due to mass transfer during primary drying, J
Ex_{in}^{pump}	exergy input in the pump, J
Ex_{loss}	exergy loss, J kg^{-1}
$Ex_{loss,t}$	total exergy loss, J kg^{-1}

Ex_{loss}^{cond} exergy losses in the condenser, J

$Ex_{loss,h}^{pd}$ exergy losses due to heat transfer during primary drying, J

$Ex_{loss,m}^{pd}$ exergy losses due to mass transfer during primary drying, J

Ex_{loss}^{pump} exergy losses in the pump, J

ΔH_s sublimation enthalpy, J kg^{-1}

J_q heat flux, W m^{-2} K^{-1}

J_w sublimation flux, kg $s^{-1}m^{-2}$

K_v heat transfer coefficient between the shelf and the product in the container, W $m^{-2}K^{-1}$

k_{dried} thermal conductivity of the dried product, W $m^{-1}K^{-1}$

k_{duct} permeability of drying chamber-condenser connection, kmol $Pa^{-1}s^{-1}$

k_{frozen} thermal conductivity of the frozen product, W $m^{-1}K^{-1}$

L_0 thickness of the product after freezing, m

L_{dried} thickness of the dried product, m

L_{frozen} thickness of the frozen product, m

M_w water molar mass, kg $kmol^{-1}$

Δm weight loss during the test to measure K_v, kg

m_p mass of the moist product, kg

$m_{w,in}$ mass of moisture in the product at the beginning of primary drying, kg

$m_{w,fin}$ mass of moisture in the product at the end of primary drying, kg

N_{cl} molar flow rate of controlled leakage, kmol s^{-1}

ΔN_{cl} ratio between the variation of the controlled leakage rate and the difference between chamber pressure and its set-point value, kmol $s^{-1}Pa^{-1}$

$N_{cl}^{t(i)}$ molar flow rate of controlled leakage at time i, kmol s^{-1}

N_{duct}	molar flow rate in the freeze-dryer duct, kmol s^{-1}
N_l	molar flow rate of leakage, kmol s^{-1}
N_{ice}	molar flow rate of water that is trapped in the condenser as ice, kmol s^{-1}
N_{pump}	flow rate of gas evacuated by the vacuum pump, kmol s^{-1}
N_v	number of vials in the batch
n	polytropic exponent of compression
n_c	total number of moles of gas in the drying chamber, kmol
n_{cond}	total number of moles of gas in the condenser chamber, kmol
$n_{w,c}$	total number of moles of water in the drying chamber, kmol
$n_{w,cond}$	total number of moles of water in the condenser chamber, kmol
P	pressure, Pa
P_0	reference pressure, Pa
P_c	chamber pressure, Pa
$P_c^{(i)}$	chamber pressure at time *i*, Pa
$P_{c,sp}$	set-point for chamber pressure, Pa
P_{cond}	condenser pressure, Pa
$P_{c,k}$	calculated value of total pressure in the drying chamber at time *k*, Pa
$P_{c,meas,k}$	measured value of total pressure in the drying chamber at time *k*, Pa
P_{out}	exhaust pressure of vacuum pumping system, Pa
p_w	partial pressure of water, Pa
$p_{w,i}$	partial pressure of water vapor at the interface of sublimation, Pa
$p_{w,i,0}$	partial pressure of water at the interface of sublimation at the beginning of the pressure rise test, Pa
$p_{w,c}$	partial pressure of water vapor in the drying chamber, Pa
$p_{w,c,0}$	partial pressure of water in the drying chamber at the beginning of the pressure

rise test, Pa

Q_{cond} heat exchanged in the vapor condenser, kJ

R ideal gas constant, J $kmol^{-1}K^{-1}$

R_p dried product resistance to vapor flow, m s^{-1}

T temperature, K

T_0 reference temperature, K

T_B product temperature at the bottom of the container, K

T_c temperature in the drying chamber, K

T_{cond} temperature in the condenser chamber, K

$T_{cooling}$ temperature of the cooling source, K

T_{des} desublimation temperature, K

T_{fluid} heating fluid temperature, K

$T_{fluid,max}$ maximum allowed heating fluid temperature, K

T_{freeze} product temperature after freezing, K

T_i product temperature at the sublimation interface, K

$T_{i,0}$ temperature of the product at the interface of sublimation at the beginning of the pressure rise test, K

$T_{in,cond}$ temperature of the vapor entering the condenser, K

T_{max} limit product temperature, K

$T_{out,cond}$ lowest temperature of ice cooled down by vapor condenser, K

t time, s

Δt duration of the test to measure K_v, s

t_d drying time, s

t_f finale time of the pressure rise test, s

t_0 initial time of the pressure rise test, s

V_c volume of the drying chamber, m^3

V_{cond} volume of the condenser chamber, m^3

x axial coordinate, m

$y_{w,c}$ water molar fraction in the drying chamber, -

$y_{w,cond}$ water molar fraction in the condenser chamber, -

$y_{w,l}$ water molar fraction in the leakage stream, -

Greeks

η exergy efficiency

ρ_{dried} apparent density of the dried product, kg m^{-3}

ρ_{frozen} density of the frozen product, kg m^{-3}

ω moisture content in the product, kg_{water} $kg_{product}^{-1}$

ω_0 moisture content in the product at the beginning of primary drying, kg_{water} $kg_{product}^{-1}$

References

Armstrong, J.G. (1980). Use of the capacitance manometer gauge in a vacuum freeze-drying. Journal of the Parenteral Drug Association, 34, 473-483.

Fissore, D., & Barresi, A.A. (2011). In-line product quality control of pharmaceuticals freeze-drying processes. In E. Tsotsas, A.S. Mujumdar (Eds.), Modern Drying Technology, Vol. 3, Wiley-VCH, Weinhein.

Fissore, D., Pisano, R., & Barresi, A.A. (2011a). Advanced approach to build the design space for the primary drying of a pharmaceutical freeze-drying process. Journal of Pharmaceutical Sciences, 100, 4922-4933.

Fissore, D., Pisano, R., & Barresi, A.A. (2011b). On the methods based on the Pressure Rise Test for monitoring a freeze-drying process. Drying Technology, 29, 73-90.

Fissore, D., Pisano, R., & Barresi, A.A. (2012). A model-based framework to optimize pharmaceuticals freeze drying. Drying Technology, 30, 946-958.

Flink, J.M. (1977). Energy analysis in dehydration processes. Food Technology, 31, 77-84.

Franks, F. (2007). Freeze-drying of pharmaceuticals and biopharmaceuticals. Royal Society of Chemistry, Cambridge.

Giordano, A., Barresi, A.A., & Fissore, D. (2011). On the use of mathematical models to build the design space for the primary drying phase of a pharmaceutical lyophilization process. Journal of Pharmaceutical Sciences, 100, 311-324.

Goff, J.A., & Gratch, S. (1946). Low-pressure properties of water from -160 to 212 °F. Transactions of the American Society of Heating and Ventilating Engineers, 52, 95-121.

Jennings, T.A. (1999). Lyophilization: introduction and basic principles. Interpharm/CRC Press, Boca Raton.

Liapis, A.I., & Bruttini, R. (2008). Exergy analysis of freeze drying of pharmaceuticals in

vials on trays. International Journal of Heat and Mass Transfer, 51, 3854-3868.

Liu, Y., Zhao, Y., & Feng, X. (2008). Exergy analysis for a freeze-drying process. Applied Thermal Engineering, 28, 675-690.

Marti, J., & Mauersberger, K. (1993). A survey and new measurements of ice vapor pressure at temperatures between 170 and 250 K. Geophysical Research Letters, 20, 363-366.

Mellor, J.D. (1978). Fundamentals of freeze-drying. Academic Press, London.

Nail, S.L., & Searles, J. (2008). Elements of Quality by Design in development and scale-up of freeze-dried parenterals. BioPharm International, 21, 44-52.

Oetjen, G.W., & Haseley P. (2004). Freeze-Drying, 2nd edn. Wiely-VHC, Weinheim.

Patel, S.M., Swetaprovo, C., & Pikal, M.J. (2010a). Choked flow and importance of Mach I in freeze-drying process design. Chemical Engineering Science, 65, 5716-5727.

Patel, S.M., Doen, T., & Pikal, M.J. (2010b). Determination of the end point of primary drying in freeze-drying process control. AAPS Pharmaceutical Science Technology, 11, 73-84.

Pikal, M.J. (1985). Use of laboratory data in freeze-drying process design: heat and mass transfer coefficients and the computer simulation of freeze-drying. Journal of Parenteral Science and Technology, 39, 115–139.

Pikal, M.J., Roy, M.L., & Shah, S. (1984). Mass and heat transfer in vial freeze-drying of pharmaceuticals: role of the vial. Journal of Pharmaceutical Sciences, 73, 1224-1237.

Pikal, M.J. (1985). Use of laboratory data in freeze-drying process design: heat and mass transfer coefficients and the computer simulation of freeze-drying. Journal of Parenteral Science and Technology, 39, 115-139.

Pisano, R., Fissore, D., Velardi, S.A., & Barresi, A.A. (2010). In-line optimization and control of an industrial freeze-drying process for pharmaceuticals. Journal of Pharmaceutical Sciences, 99, 4691-4709.

Pisano, R., Fissore, D., & Barresi, A.A. (2011a). Freeze-drying cycle optimization using model predictive control techniques. Industrial & Engineering Chemistry Research, 50, 7363-7379.

Pisano, R., Fissore, D., & Barresi, A.A. (2011b). Heat transfer in freeze-drying apparatus. In M.A. dos Santos Bernardes (Ed.), Developments in Heat Transfer. Rijeka, InTech.

Pisano, R., Fissore, D., Barresi, A.A., Brayard, P., Chouvenc, P., & Woinet, B. (2013). Quality by Design: optimization of a freeze-drying cycle via design space in case of heterogeneous drying behavior and influence of the freezing protocol. Pharmaceutical Development and Technology, 18, 280-295.

Ratti, C. (2001). Hot air and freeze-drying of high-value foods: a review. Journal of Food Engineering, 49, 311–319.

Sane, S.U., Hsu, C.C. (2008). Mathematical model for a large-scale freeze-drying process: A tool for efficient process development & routine production. In B.N. Thorat, A.S. Mujumdar (Eds.), Drying 2008 - Proceedings of 16th International Drying Symposium, November 9-12, Ramoji Film City (Hyderabad), India, Vol. B, 680-688.

Searles, J. (2004). Observation and implications of sonic water vapour flow during freeze-drying. American Pharmaceutical Review, 7, 58-69.

Sheehan, P., & Liapis, A.I. (1998). Modeling of the primary and secondary drying stages of the freeze drying of pharmaceutical products in vials: numerical results obtained from the solution of a dynamic and spatially multidimensional lyophilization model for different operational policies. Biotechnology and Bioengineering, 60, 712–728.

Velardi, S.A., & Barresi, A.A. (2008). Development of simplified models for the freeze-drying process and investigation of the optimal operating conditions. Chemical Engineering Research and Design, 87, 9-22.

Wagner, W., Saul, A., & Pruss, A. (1994). International equations for the pressure along the

melting and along the sublimation curve of ordinary water substance. Journal of Physical and Chemical Reference Data, 23, 515-527.

List of Tables

List of Figures

condensing (graph B) as a function of chamber pressure and heating fluid temperature (o: T_{fluid} = -20°C, □: T_{fluid} = -10°C, Δ: T_{fluid} = 0°C).

Figure 7: Values of the total exergy loss during the primary drying step as a function of chamber pressure (graph A, ○: T_{fluid} = -20°C, □: T_{fluid} = -10°C, Δ: T_{fluid} = 0°C) and of heating fluid temperature (graph B, ●: P_c = 5 Pa, ■: P_c = 10 Pa, ▲: P_c = 20 Pa).

Figure 8: Values of the exergy yield as a function of the operating conditions (dotted curves). Solid line identifies the design space when L_{dried}/L_0 = 0.5.

Table 1

Drying chamber volume (V_c)	0.178 m^3
Condenser chamber volume (V_{cond})	0.1 m^3
Controlled leakage rate for pressure control (ΔN_{cl})	$1.0 \cdot 10^{-10}$ kmol $Pa^{-1}s^{-1}$
Leakage rate (N_l)	$4.97904 \cdot 10^{-10}$ kmol s^{-1}
Total sublimation area (A_{sub})	0.16 m^2

Table 2

Condenser pressure, Pa	0.0	0.2	0.3	0.5	0.7	0.8	1.0	2.0	3.0	5.0	20.0	10^3	10^4
Pump flow rate, $m^3 h^{-1}$	0.0	0.1	0.4	2.0	4.8	5.8	7.0	9.5	11.0	13.0	15.0	18.0	19.0

Figure 1

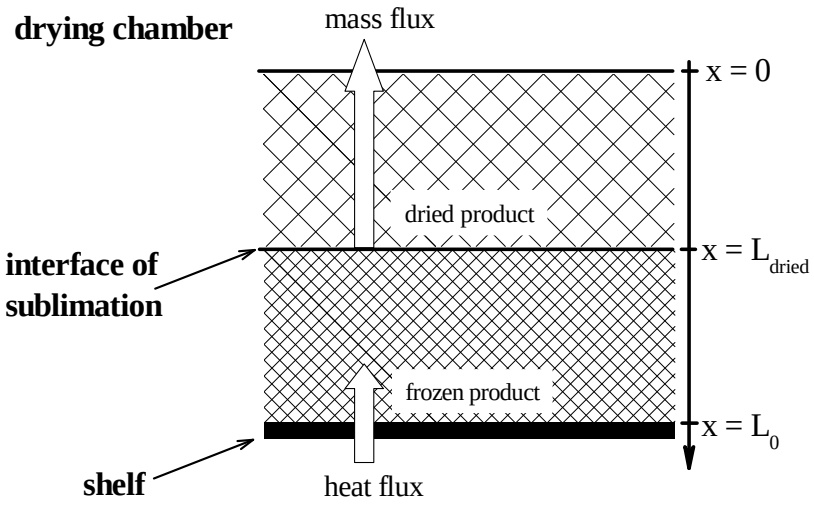
drying chamber
mass flux
x = 0
dried product
interface of sublimation
x = L dried
frozen product
x = L 0
shelf
heat flux

Figure 2

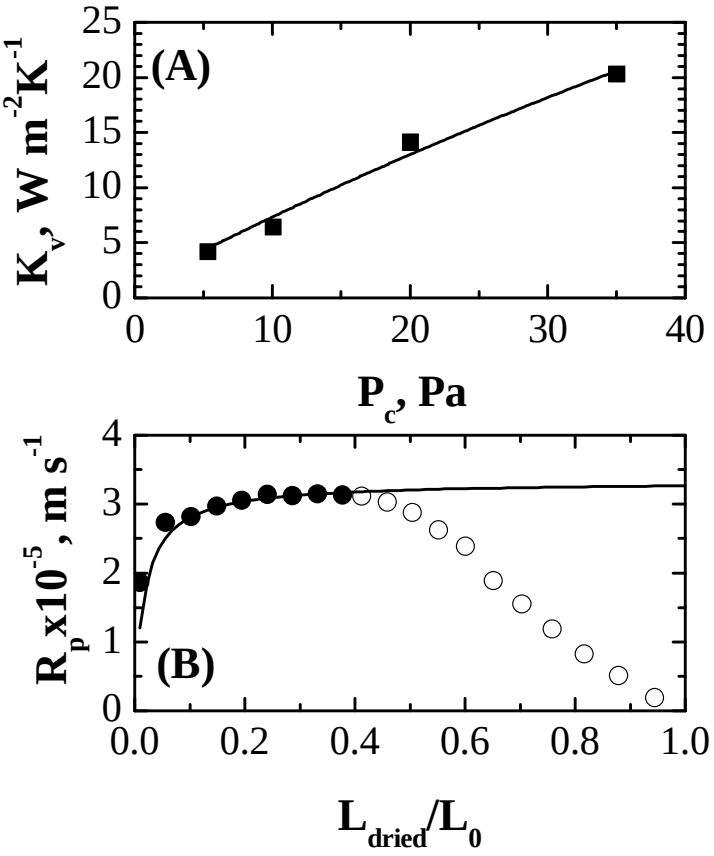
(A)
K_v, W m^{-2}K^{-1}
0
5
10
15
20
25
0
10
20
30
40
P_c, Pa
(B)
R_p x10^{-5}, m s^{-1}
0
1
2
3
4
0.0
0.2
0.4
0.6
0.8
1.0
L_{dried}/L_0

Figure 3

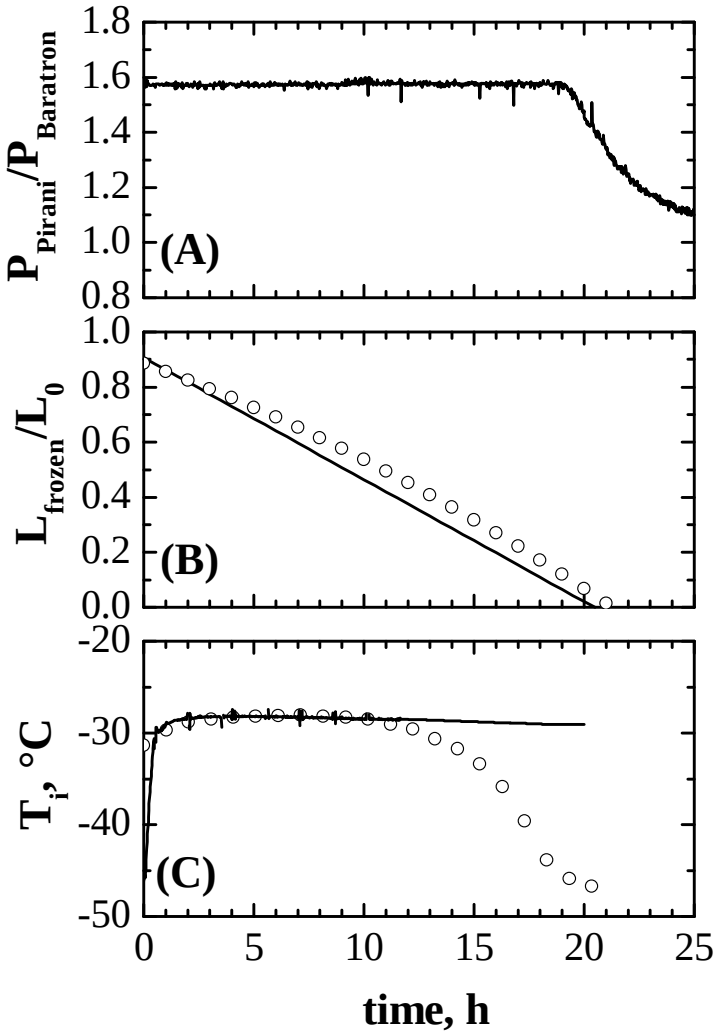
1.8
1.6
1.4
1.2
1.0
0.8
$P_{Pirani}/P_{Baratron}$
(A)
1.0
0.8
0.6
0.4
0.2
0.0
L_{frozen}/L_0
(B)
-20
-30
-40
-50
T_i, °C
(C)
0
5
10
15
20
25
time, h

Figure 4

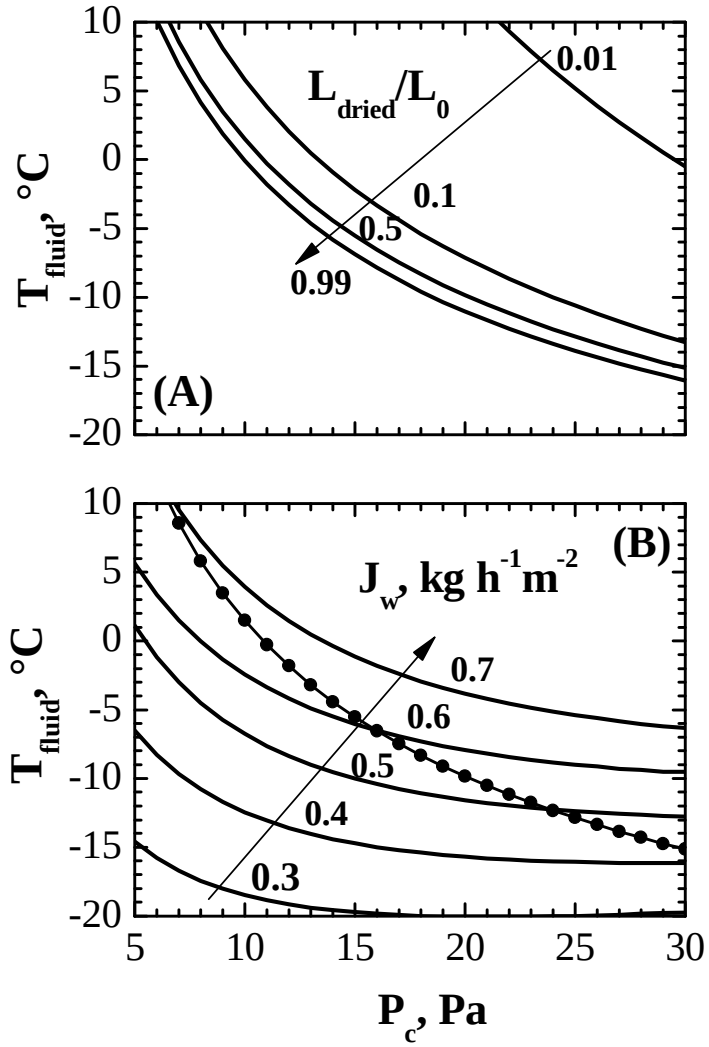
10
5
0
-5
-10
-15
-20
T_{fluid}, °C
L_{dried}/L_0
0.01
0.1
0.5
0.99
(A)
J_w, kg $h^{-1}m^{-2}$
(B)
0.7
0.6
0.5
0.4
0.3
5
10
15
20
25
30
P_c, Pa

Figure 5

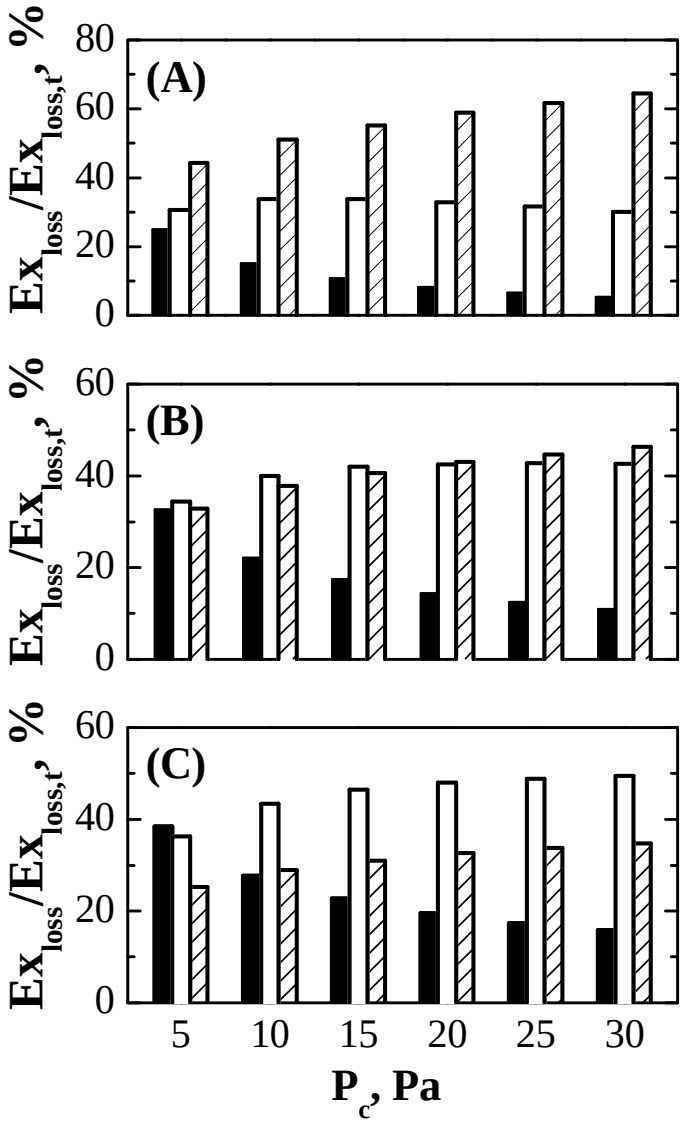

Figure 6

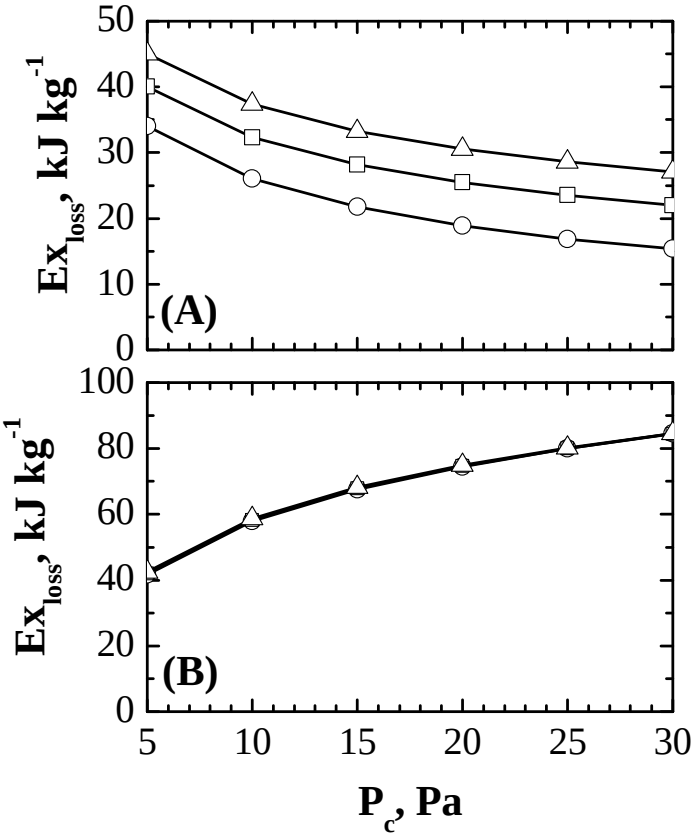
50
40
30
20
10
0
Ex_{loss}, kJ kg^{-1}
(A)
100
80
60
40
20
0
Ex_{loss}, kJ kg^{-1}
(B)
5
10
15
20
25
30
P_c, Pa

Figure 7

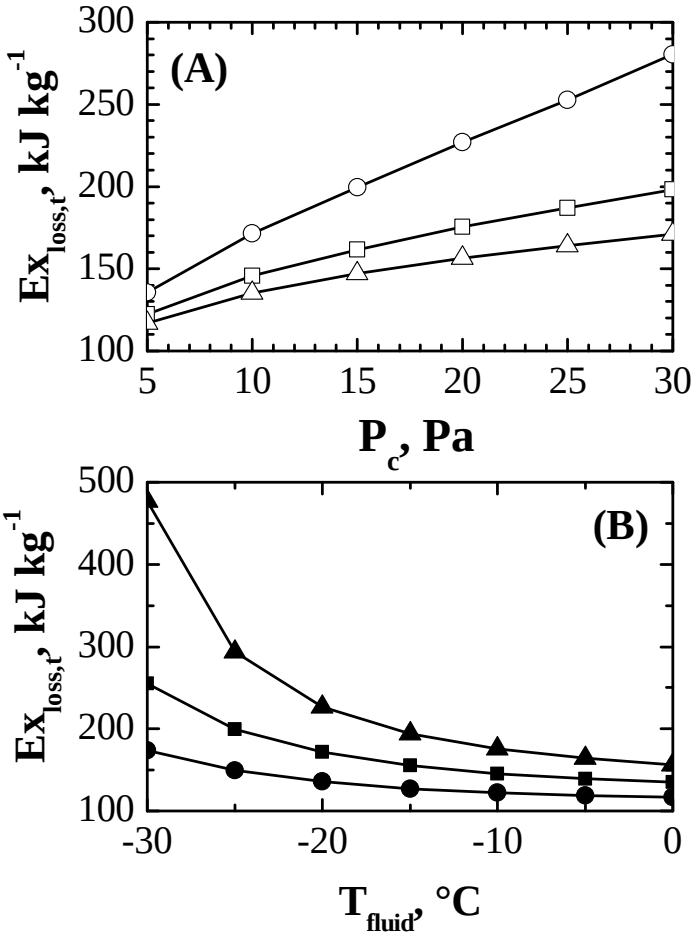
(A)
$Ex_{loss,t}$, kJ kg^{-1}
300
250
200
150
100
5
10
15
20
25
30
P_c, Pa
(B)
$Ex_{loss,t}$, kJ kg^{-1}
500
400
300
200
100
-30
-20
-10
0
T_{fluid}, °C

Figure 8

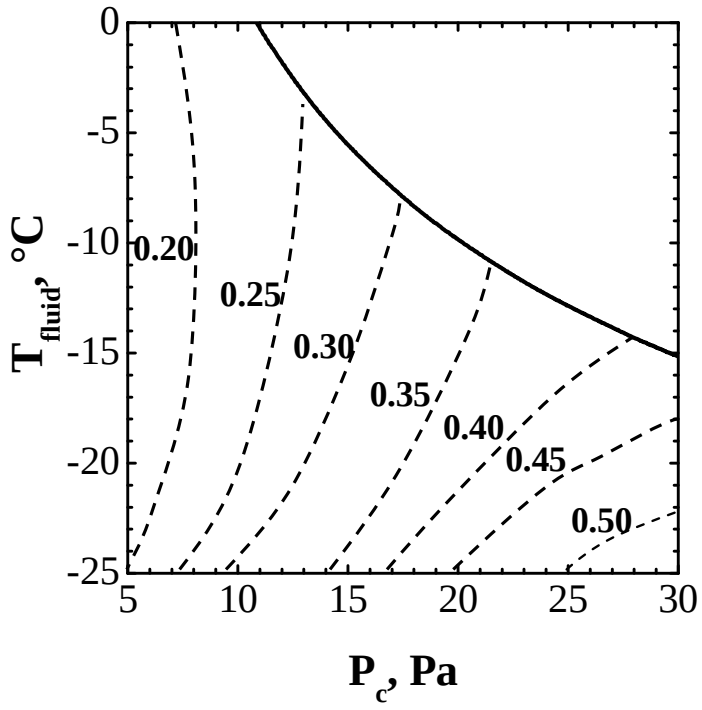
0
-5
-10
-15
-20
-25
5
10
15
20
25
30
T_{fluid}, °C
P_c, Pa
0.20
0.25
0.30
0.35
0.40
0.45
0.50